J. Mt. Sci. (2013) 10(3): 482–493
DOI: 10.1007/s11629-013-2345-x

Permeability and Sedimentation Characteristics of Pleistocene Fluvio-glacial Deposits in the Dadu River Valley, Southwest China

TU Guo-xiang[1], HUANG Run-qiu*[1], DENG Hui[1], LI Yan-rong[2]

1 State Key Laboratory of Geo-hazard Prevention and Geo-environment Protection, Chengdu University of Technology, Chengdu 610059, China

2 Department of Earth Sciences, The University of Hong Kong, Hong Kong, China

**Corresponding author, e-mail: hrq@cdut.edu.cn; First author, e-mail: pyk@cdut.edu.cn*

Abstract: There exist many fluvio-glacial deposits in the valley of Dadu River, Southwest China, which dates back to the Pleistocene. As some of the deposits are located within the seasonal water fluctuation zone of reservoirs, the seepage of groundwater acts as one of the key factors influencing their stability. Investigation into the sediment properties and permeability is, therefore, crucial for evaluating the sediment stability. In this study, in-situ permeability and sieving tests have been carried out to determine grain size distribution, correlations of permeability and hydraulic gradients, and relations between permeability and sedimentation properties. Test results indicate that the deposits are composed mostly of sands, gravels, cobbles and boulders, and the percentage of fines is less than 5%. The sediments have high densities, low porosities and natural moisture contents. At low hydraulic gradients, the seepage velocity obeys the Darcy's law, while a non-Darcy permeability is observed with hydraulic gradient exceeding a certain value (about 0.5 - 0.7). The linear permeability coefficient ranges from 0.003 to 0.009 cm/s. Seepage failure occurs above a threshold between 1.1 and 1.5. The test data fit well with the non-linear permeability equations suggested by Forchheimer and Izbash. The non-Darcy permeability proves to be in accordance with the seepage equation suggested by Izbash with the power 'm' of about 0.6 - 0.7. The characteristic grain sizes of the studied deposits are found in a narrow range between 0.024 and 0.031 mm, which is much lower than the effective grain size (d_{10}).

Keywords: Fluvio-glacial deposits; Grain size distribution; Linear and non-linear permeability; Seepage failure

Introduction

Six major glaciations likely occurred in Southwest China during the Marine Oxygen Isotope Stages (MIS-16, MIS-14/12, MIS-6, MIS-3, and early MIS-2) and the global Last Glacial Maximum (Xu and Zhou 2009; Yi et al. 2005). During melting periods large amounts of loose materials were transported and deposited in valleys by melt water forming fluvial glacial deposits in the valley of the Dadu River, Southwestern China (Zheng 2001; Wang 2006; Xu 2010; Tu et al. 2012).

Fan deposits in front of continental glaciers are generally composed of sands, silts and clays (Kjaer et al. 2004; Knight 2009; Kneller et al. 2004; Smerdona et al. 2005; Blažauskas et al. 2007), while outwash materials deposited in front of valley-type glaciers contain lots of gravels, cobbles and boulders (Knight 1999; Smith 2004; Heinz et al. 2003; Hobbs 1931). Previous investigations by the authors revealed that outwash materials in the valley of the Dadu River mainly contain sands, gravels, cobbles and boulders, and the weight percentage of fines (< 0.075 mm) is normally less

Received: 9 March 2012
Accepted: 5 March 2013

than 5%. They are normally poorly sorted and show high densities, low porosities and low natural moisture contents (Tu et al. 2010; Tu 2010).

Some publications reported only permeability under low hydraulic gradients (e.g., 0.1 - 0.5) (Salem 2001; Heinz et al. 2003; Smerdona et al. 2005), and few articles discussed constitutive equations for the permeability of the outwash deposits (Tu et al. 2010). Few researches have been done on the permeability of outwash deposits in the study area. Since the non-Darcy flow of porous media was found by Forchheimer in 1901, scholars have studied various nonlinear soil permeability (Izbash 1931; Basak 1976; Bordier and Zimmer 2000; Venkataraman and Rao 2000). These studies concluded that the Darcy's law is only valid for soils at a low hydraulic gradient.

Most outwash deposits in the Dadu River valley are located in the seasonal water table fluctuations in the vicinity of hydropower stations, the Yingliangbao and the Pubugou hydropower stations for example (Table 1). They are alternatively submerged or exposed partly/wholly with fluctuation of reservoir water table. The seepage of groundwater is therefore one of the crucial factors influencing the stability of the deposits, especially during water table fluctuation. Failure of these deposits might cause fatalities and economic losses due to the huge volumes (most of them exceed millions cubic meters and some even exceed ten millions). Failure of Deposit 1 (Table 1), for instance, would destroy the expressway across the deposit and failure of Deposit 4 (Table 1) would threaten the security of Yingliangba hydropower station located 1,000 m downriver from the deposit. Study on the permeability of these deposits is considered to be an important complement for evaluating their stability, especially in the period of fluctuation of reservoir water. The present study takes four representative fluvio-glacial deposits (Figure 1 and Table 1) as example to achieve this.

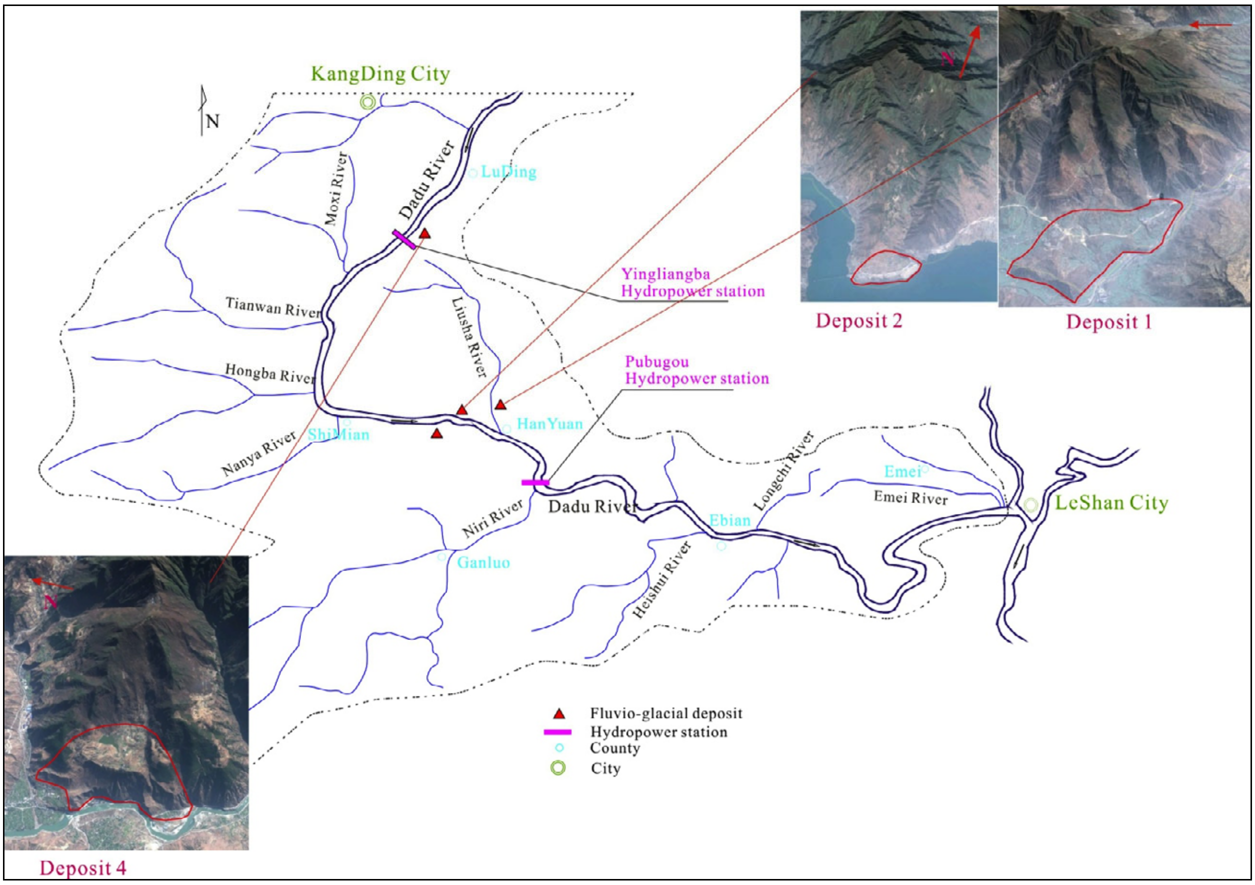

Figure 1 Study area and locations of the studied fluvio-glacial deposits in Sichuan Province, China

Table 1 General information of the studied fluvio-glacial deposits

Deposit	Location	Fluctuation range of water table (above sea level)	Altitude of deposits	Volume (10^6 m^3)
1	left bank of the Liusha river Pubugou hydropower station reservoir	790 - 850 m	810 - 930 m	200
2	left bank of the Dadu River Pubugou hydropower station reservoir	790 - 850 m	790 – 1,200 m	57
3	right bank of the Dadu River Pubugou hydropower station reservoir	790 - 850 m	800 – 1,100 m	10
4	left bank of Dadu River Yingliangba hydropower station reservoir	1,230 – 1,246 m	1,220 – 1,440 m	44

1 Study Area

The Dadu River, located in the west of Sichuan Province, China, originates from the Bayanhar Mountain seated in Qinghai Province. It is about 1,155 km long and characterized as a high-mountain, deep-canyon river with steep bank slopes. Liu et al. (2007) and Xiong et al. (2009) suggested that the Dadu River was formed in Middle Pleistocene. The mountain glaciers were considered to be formed along both sides of the Dadu River during the Pleistocene glaciation in West China, while sediments were transported by intermittent melting glaciers, forming the current fluvio-glacial deposits (Shi 2002; Yi et al. 2005; Luo and Yang 1963; Liu et al. 1986; Zheng 2001; Wang 2006; Xu 2010; Tu et al. 2012). The deposits investigated in this paper are located in the middle stream of the Dadu River, between Hanyuan and Luding towns (Figure 1). The U-shaped valleys formed by glacial erosion are typical in the study area.

The basic information of the studied deposits is listed in Table 1. Each deposit has a gentle platform dipping at 5° - 15°, in front of which a steep bank slope dips at 60° - 70° towards the river. Deposits 1, 2 and 3 are located in the Reservoir of the Pubugou hydropower station, and Deposit 4 is located in the Reservoir of the Yingliangbao hydropower station. They all will be submerged partly when the water level in the reservoir rises up.

2 Methods

According to initial investigation by the authors (Tu et al. 2010; Tu et al. 2012), the deposits are composed mainly of coarse soil (coarse fraction is over 50%) and very coarse soil (very coarse fraction is over 55%). The coarse soils, distributed at the bottom of the deposits, are composed mainly of well-bedded gravels and sands, sub-rounded and well-sorted. The very coarse soils are composed mainly of poorly-bedded gravels and cobbles, non-sorted and sub-rounded.

In this study, 3 - 5 representative testing locations were selected for each deposit. A 1 m × 1 m × 1 m pit was dug at each test location. Samples were collected from both coarse soil layer and very coarse soil layer, and sieve tests were carried out afterwards. Before the sieve test, particles greater than 60 mm in diameter were measured by ruler or vernier caliper and divided into four fractions: > 200 mm, 200 - 100 mm, 100 - 80 mm and 80 - 60 mm. The remaining part of the sample (< 60 mm) was split into ten fractions: 60 - 40 mm, 40 - 20 mm, 20 - 10 mm, 10 - 5 mm, 5 - 2 mm, 2 - 1 mm, 1 - 0.5 mm, 0.5 - 0.25 mm, 0.25 - 0.075 mm and < 0.075 mm. The weight percentage of each fraction was calculated to construct the grain size distribution curves (Figures 2 and 3). As most of the deposits show a certain degree of argillaceous or calcareous cementation, much effort were paid to prevent the breakage of coarse particles. Three parameters, particle specific gravity (Gs), natural moisture content (w) and natural density (ρ), were obtained according to the Chinese Test Methods of Soils for Highway Engineering (JTG E40 - 2007).

Methods for testing soil permeability can be carried out in two ways, laboratory and in-situ. The former includes constant head and variable head permeability tests. The latter mainly includes bore pumping-in, single-ring pit pumping-in and double-ring pit pumping-in tests. Laboratory tests produce relationships of seepage velocity against hydraulic gradient, which present a complete view of the soil permeability. However, it is usually difficult to obtain a precise relationship between seepage velocity and hydraulic gradient from in-situ tests. Furthermore, the small size of laboratory

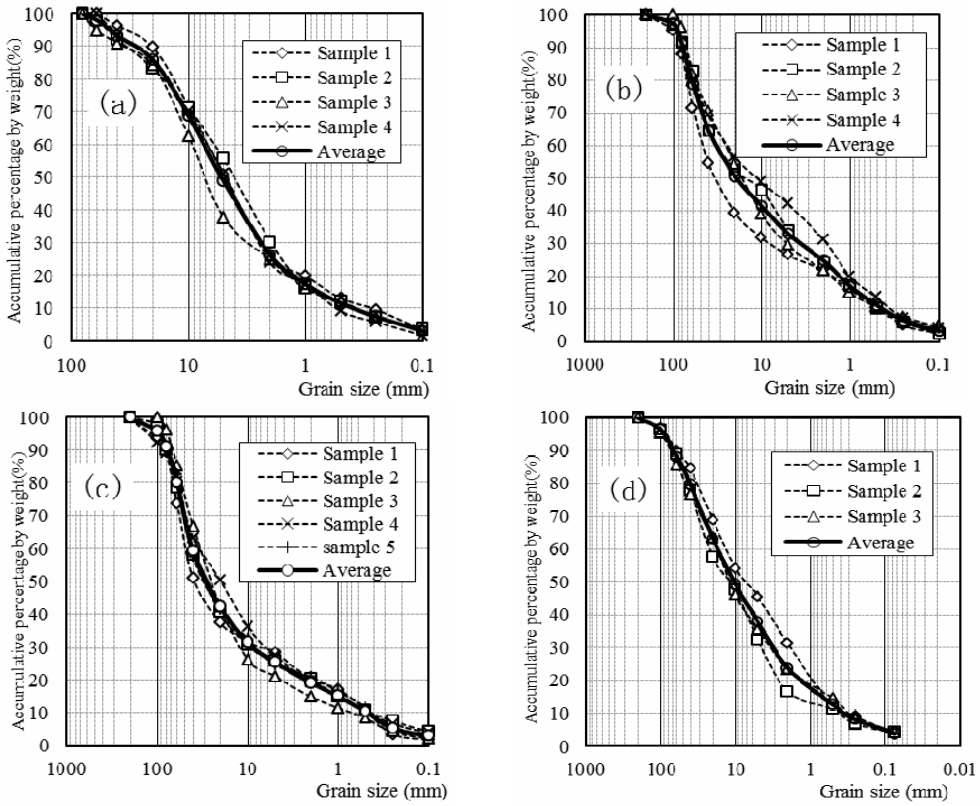

Figure 2 Grain-size distribution of coarse soil: (a) Deposit 1; (b) Deposit 2; (c) Deposit 3; and (d) Deposit 4

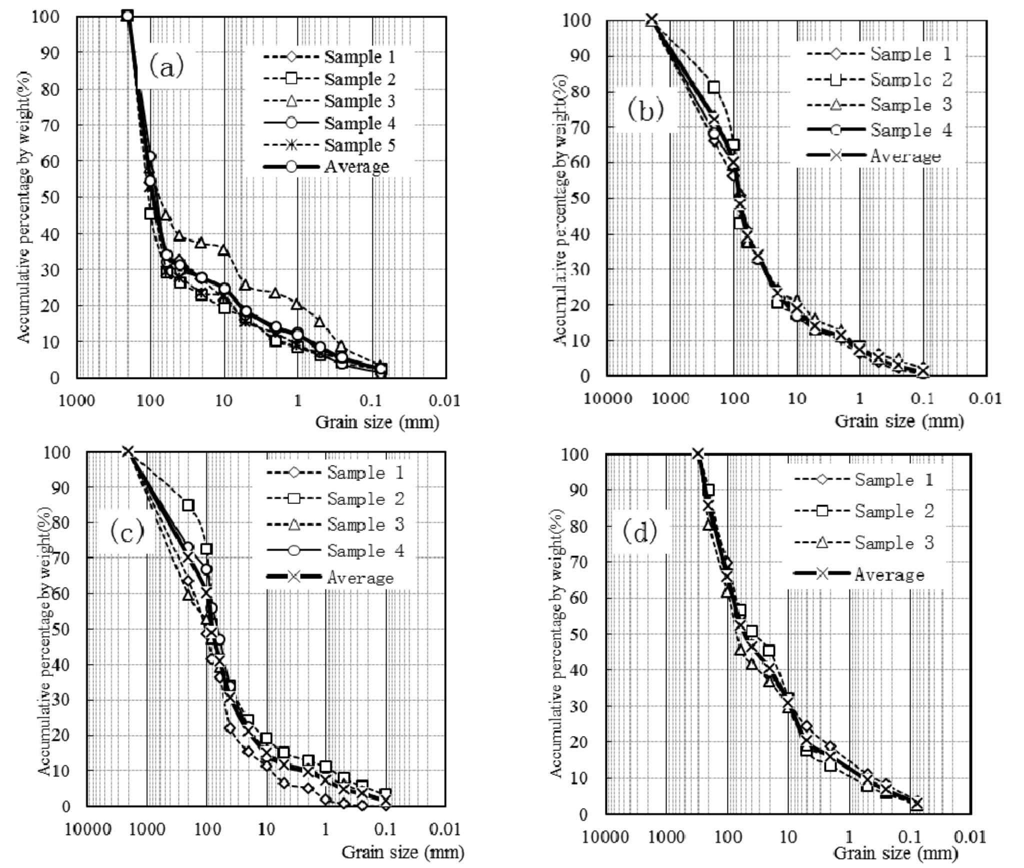

Figure 3 Grain-size distribution of very coarse soil: (a) Deposit 1; (b) Deposit 2; (c) Deposit 3; and (d) Deposit 4

equipment does not allow testing coarse soils.

For testing the studied deposits, a special in-situ permeability test was designed similar to the vertical permeability test in laboratory. The sample chamber with a diameter of 1 m allows testing samples containing particles smaller than 300 mm. Six steps are needed to perform this test: 1) select a representative test point in each coarse soil layer and very coarse soil layer; 2) dig a soil column with a height of 1.6 m and a diameter of 1 m; 3) wrap the soil column with cement mortar of 5 cm thick; 4) install a water intake storage tank with a height of 20 cm and a diameter of 1 m, made of steel, at the top of the soil column (be sure that the storage is closely cemented and embedded at least 10 cm into the cement package); 5) cut off the bottom of the wrapped soil column when the cement mortar achieves enough strength; and 6) invert the soil column and install the water outlet storage (height of 25 cm and diameter of 1 m) at the other end of the soil column (Figure 4).

The test set-up is shown in Figure 4 and the test procedures are given as follows:

(1) Connect water tank with water intake storage, open the drain tap and the inlet valve, while close the drain tap when water flows out from it;

(2) Saturate the sample by keeping water flowing out from Outfall 1 for 24 hours;

(3) Keep the water head constant and record water heads, seepage time, flux and turbidity of the water flowing out from the outfall at every 30 minute;

(4) Draw the hydraulic gradient and seepage velocity curves during the test;

(5) When the seepage velocity increases suddenly or the water flowing out shows some turbidity, end the test; and

(6) Repeat steps 3 through 5 for different hydraulic gradients.

3 Results

3.1 Grain size distribution

According to the test results of 32 samples from the four studied deposits, the soils can be divided into two groups, one is typical coarse soil or coarse soil with cobbles and the other is very coarse soil. As shown in Figure 5, the coarse soil is composed mainly of gravels (diameter of 2 - 60 mm, weight percentage greater than 50%), sands (0.075 - 2 mm, 25 - 35%) and cobbles (60 - 200 mm, 10% - 20%), and fines (< 0.075 mm, < 5%). Very coarse soil is composed mostly of gravels,

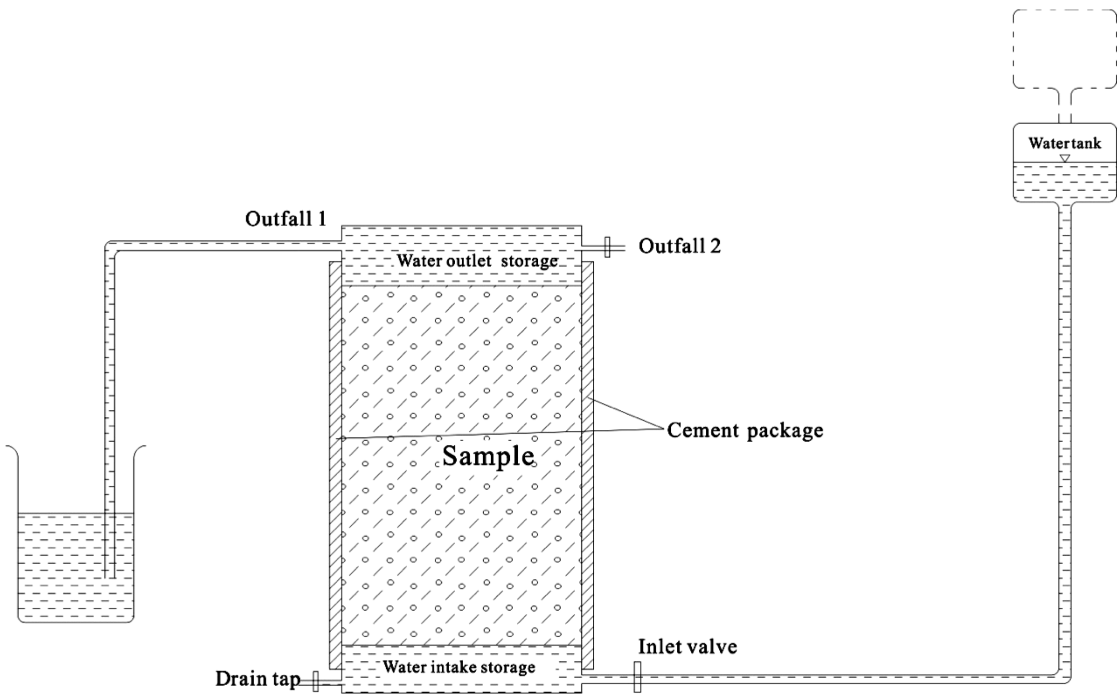

Figure 4 Layout of the test set-up

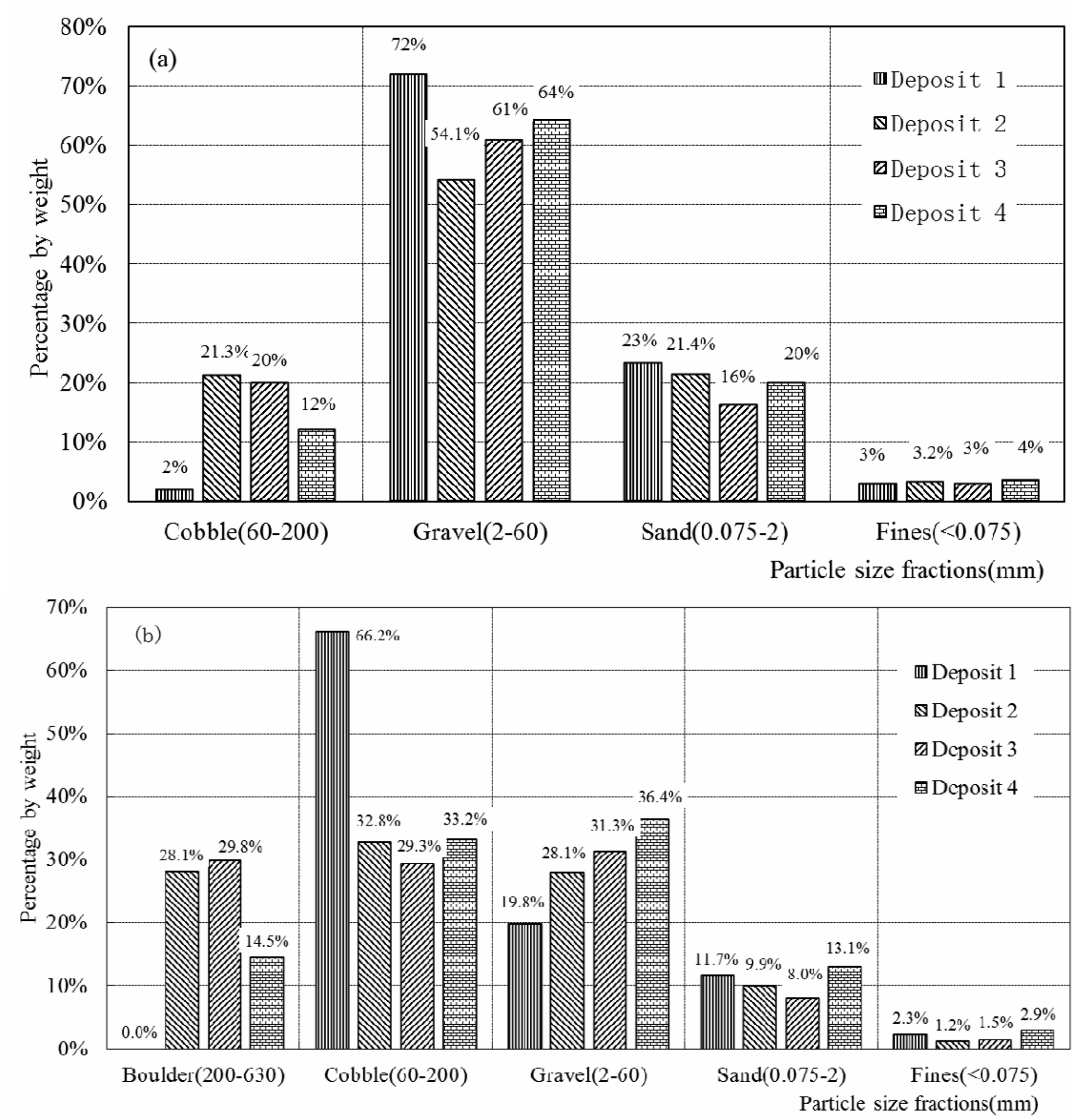

Figure 5 Weight percentage of sub-fractions: (a) Coarse soil; and (b) Very coarse soil

cobbles and boulders (>200 mm), and the total percentage of these three fractions is greater than 85%, in which the boulders and rocks fragments account for about 55% while fines less than 3%.

The grain size distribution curves are shown in Figure 2, and distribution parameters (d_{10}, d_{30}, d_{50}, etc.) are given in Table 2. The values of d_{10} and d_{30} for coarse soils fall in a narrow range (d_{10}: 0.36 mm - 0.48 mm, d_{30}: 2.51 mm - 8.84 mm), while the values of d_{50} and d_{60} show much larger variations (d_{50}: 5.33 mm - 28.94 mm, d_{60}: 7.81 mm - 40.67 mm). The coefficient of non-uniformity C_u (d_{60}/d_{10}) ranges between 19.05 and 84.73, and the coefficient of curvature C_c ($d_{30}^2/(d_{60}\times d_{10})$) is between 1.04 and 4.0. This indicates that the coarse soil in the four studied deposits is classified as poorly sorted but well graded.

Figure 3 shows the grain size distribution of the very coarse soils and Table 3 shows the typical particles sizes of very coarse soils. The variation of d_{10} and d_{30} are larger than that of coarse soils with d_{10} about 0.64 mm - 2.75 mm and d_{30} about 9.6 mm - 39.05 mm. However the variation of d_{50} and d_{60} of very coarse soils are less than that of coarse soils with d_{50} about 52.29 mm - 91.69 mm and d_{60} 82.57 mm - 125.17 mm. C_u value ranges between 36.32 and 169.15, and C_c between 1.74

Table 2 Grain size parameters of coarse soil

Deposit	Sample No.	d_{60}	d_{50}	d_{30}	d_{10}	d_{60}/d_{10}	$d^2_{30}/(d_{60}\times d_{10})$
1	1	7.22	4.93	2.49	0.56	12.89	1.53
	2	6.45	4.35	1.98	0.40	16.13	1.52
	3	9.48	7.49	3.24	0.40	23.95	2.80
	4	7.35	4.88	2.67	0.56	13.10	1.73
	Average	7.81	5.33	2.51	0.41	19.05	1.97
2	1	46.71	34.32	8.44	0.52	89.83	2.93
	2	32.73	16.10	3.79	0.49	67.07	0.90
	3	27.36	17.37	5.37	0.46	59.48	2.29
	4	25.71	11.79	1.91	0.37	69.49	0.38
	Average	33.58	19.48	3.96	0.45	74.62	1.04
3	1	47.92	38.69	7.61	0.47	102.83	2.59
	2	41.87	30.74	9.58	0.44	94.30	4.94
	3	34.40	26.17	12.33	0.76	45.38	5.83
	4	34.84	19.65	6.44	0.47	74.60	2.55
	5	42.06	30.81	8.42	0.44	96.03	3.85
	Average	40.67	28.94	8.84	0.48	84.73	4.00
4	1	14.04	7.64	3.42	0.33	42.54	2.52
	2	22.66	12.47	4.56	0.43	52.70	2.13
	3	18.20	12.38	3.62	0.31	58.71	2.32
	Average	17.81	10.58	3.34	0.36	49.47	1.74

Table 3 Grain size parameters of very coarse soil

Deposit	Sample No.	d_{60}	d_{50}	d_{30}	d_{10}	d_{60}/d_{10}	$d^2_{30}/(d_{60}\times d_{10})$
1	1	125.71	91.80	30.64	1.65	76.19	4.53
	2	154.01	117.52	62.47	1.83	84.02	13.82
	3	109.07	75.45	7.24	0.30	363.57	1.60
	4	98.50	84.85	42.86	0.79	124.68	23.61
	5	130.87	95.36	61.03	1.30	100.67	21.89
	Average	125.17	91.69	33.55	0.74	169.15	12.15
2	1	142.27	78.86	31.72	2.05	69.40	3.45
	2	95.62	86.48	34.14	1.64	58.30	7.43
	3	107.97	82.72	33.26	1.47	73.45	6.97
	4	107.87	81.02	33.70	1.79	60.26	5.88
	Average	102.30	83.57	33.38	1.72	59.48	6.33
3	1	175.53	108.87	51.15	8.65	20.29	1.72
	2	88.25	77.45	31.88	0.86	102.62	13.39
	3	226.60	90.19	35.64	1.86	121.83	3.01
	4	87.78	66.97	33.51	1.96	44.79	6.53
	Average	99.87	81.90	39.05	2.75	36.32	5.55
4	1	73.62	47.77	9.26	0.41	179.11	2.83
	2	74.02	39.79	9.31	1.22	60.67	0.96
	3	95.83	71.29	10.69	0.61	157.10	1.95
	Average	82.57	52.29	9.60	0.64	129.02	1.74

and 12.15. Thus, the very coarse soils of the four deposits are of poorly-sorted and poorly-graded sediments.

3.2 Sedimentation characteristics

Three main physical parameters (G_s, w, and ρ) of the outwash deposits were obtained from 16 samples, and the porosity ratio, e, was calculated as listed in Table 4, which indicates that the soils

Table 4 Physical parameters

Deposit	Soil type	G_s	W (%)	ρ (kg·m^{-3})	e
1	①	2.65	8	2.33	0.23
	②	2.65	9.62	2.32	0.25
2	①	2.64	8.85	2.26	0.24
	②	2.65	8.93	2.27	0.27
3	①	2.66	9.66	2.24	0.3
	②	2.64	8.38	2.3	0.25
4	①	2.68	15.6	2.15	0.43
	②	2.67	12.97	2.18	0.38

Note: ① - coarse soil; and ② - very coarse soil

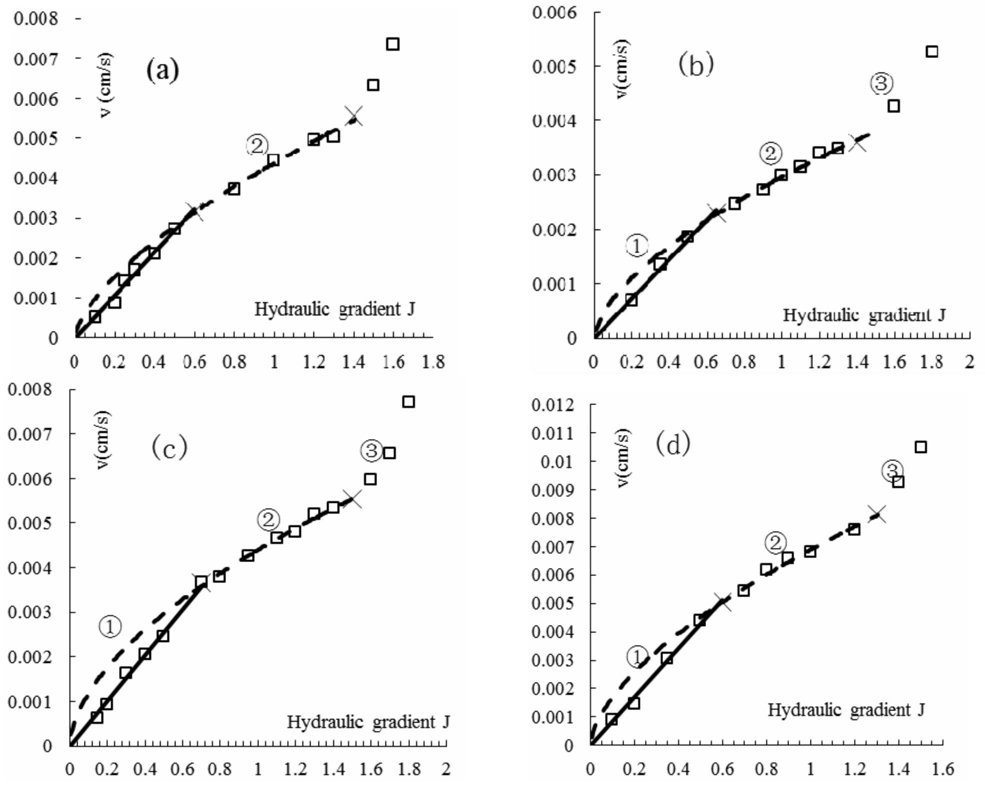

Figure 6 Relation between hydraulic gradient and seepage velocity of coarse soils: (a) Deposit 1; (b) Deposit 2; (c) Deposit 3; and (d) Deposit 4

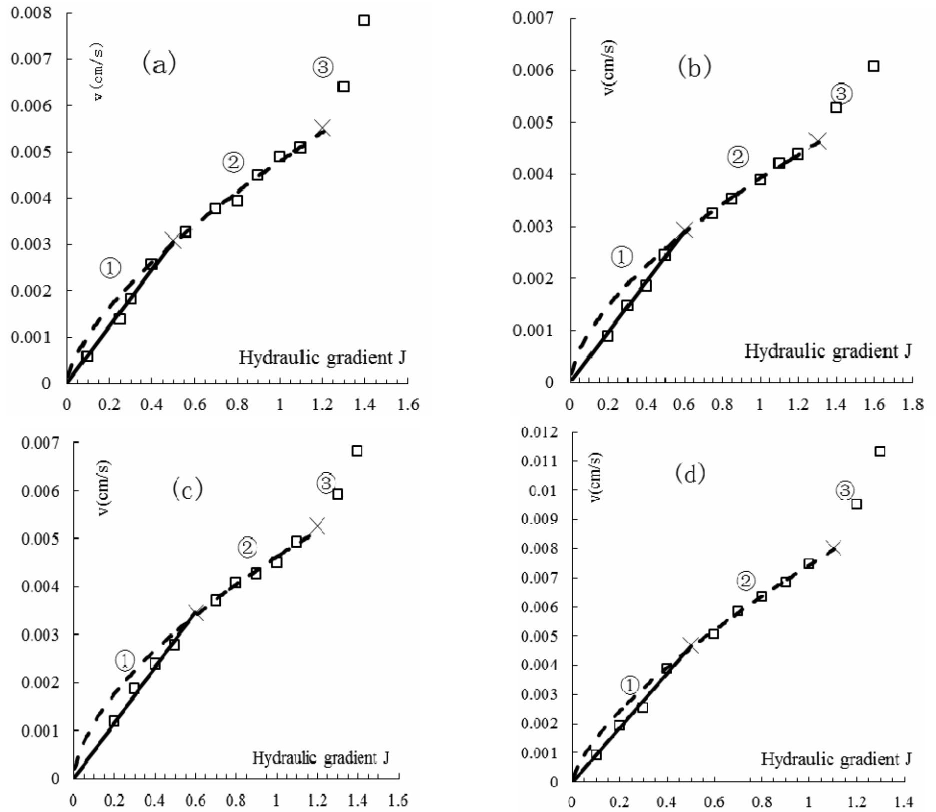

Figure 7 Relation between hydraulic gradient and seepage velocity of very coarse soils: (a) Deposit 1; (b) Deposit 2; (c) Deposit 3; and (d) Deposit 4

have high densities, low porosities and low natural moisture content. For the coarse soils, G_s lies in a narrow range between 2.64 and 2.68, w between 8% and 15.6%, ρ between 2.15 kg·m^{-3} - 2.33 kg·m^{-3}, and e between 0.23 and 0.43. For the very coarse soils, G_s ranges between 2.64 and 2.67, ρ 2.18 kg·m^{-3} - 2.32 kg·m^{-3}, w 8.38% - 12.97%, and e 0.25 - 0.38.

3.3 Permeability

3.3.1 Coarse soils

Figure 6 shows curves of hydraulic gradient vs. seepage velocity of the coarse soils. The curves can be divided into three parts: 1) a linear relationship at low hydraulic gradient, 2) a nonlinear trend at intermediate hydraulic gradient, and 3) a nonlinear trend at high hydraulic gradient. Above a certain threshold, the knickpoint as shown in Figure 6, the seepage velocity increases faster than gradient. In the meantime, the water flowing out from the outlet is observed to contain fines with turbidity, indicating seepage failure of the sample.

According to the test results, the hydraulic gradient thresholds, where the seepage turns from linear to nonlinear, are 0.6, 0.65, 0.7, 0.6 and the hydraulic gradient thresholds of seepage failure are 1.4, 1.4, 1.5 and 1.3 for a, b, c and d samples, respectively. The linear permeability coefficients, obtained from Darcy's law, of the four studied deposits are 0.0054, 0.0036, 0.0044 and 0.0085 cm/s, respectively.

3.3.2 Very coarse soils

Like coarse soils, the seepage curves (hydraulic gradient vs. seepage velocity) of very coarse soils can be divided into three phrases (Figure 7). It obeys Darcy's law, until the hydraulic gradient exceeds a certain threshold. Again, there exists a knick point indicating seepage failure. The thresholds for the hydraulic gradient to change from linear seepage to nonlinear seepage are 0.5, 0.6, 0.7, 0.5 and the hydraulic gradient thresholds of seepage failure are 1.2, 1.3, 1.2, and 1.1 for a, b, c and d samples, respectively. The linear permeability coefficients of very coarse soils calculated by Darcy's law are 0.0061, 0.0048, 0.0058, and 0.0093 cm/s, respectively. The threshold for seepage failure is normally higher than that for coarse soils.

4 Discussion

4.1 Permeability equations

Since Darcy's linear permeability law, researchers in this filed have explored soil's seepage constitutive relations in various forms, including both linear and non-linear relationships (Forchheimer 1901, Izbash 1931, Hanbo 1973, Lesaffre 1988). Among them the most famous non-linear equations (Equation 1) were proposed by Forchheimer (1901):

$$\begin{aligned} &J = av + bv^2 \\ &a = \mu / gk_0, b = \beta\rho \end{aligned} \tag{1}$$

where J (dimensionless) is the hydraulic gradient; a (s/m) and b (s^2/m^2) are coefficients related to properties of medium and fluid; μ (m^2/s) kinematic viscosity of the fluid; k_0 (m^2) intrinsic permeability; β (m.s^2/kg) the non-Darcy coefficient; ρ (kg/m^3) the fluid density; υ (m/s) velocity; and g (m/s^2) acceleration of gravity.

According to Poiseuille's law (Wang et al. 2009), υ can be written as:

$$v = \frac{\rho g R^2}{8\upsilon} J = k_0 \frac{\rho g}{\upsilon} J \tag{2}$$

then:

$$k = k_0 \frac{\rho g}{\upsilon}, \upsilon = \mu\rho \tag{3}$$

where k (m/s) is the permeability coefficient; υ (Pa·s) viscosity of fluid; and R (m) radius of tube.

Based on Equations 1 and 3, there is:

$$k = \frac{1}{a} \tag{4}$$

Izbash (1931) proposed the following relationship:

$$v = k_w J^m \tag{5}$$

where k_w is the general permeability coefficient (m/s).

In the present study, linear and non-linear regressions are carried out for the first and second parts as shown in Figures 6 and 7. Table 5 shows the results and gives linear seepage equation and the hydraulic gradient thresholds.

Figures 6 and 7 indicate that the permeability is in good agreement with Darcy's law at low hydraulic gradients. However, for hydraulic gradients greater than 0.6 - 0.7 in coarse soils and greater than 0.5 - 0.6 in very coarse soils, the seepage exhibits non-Darcy characteristics. In the case of coarse soils, linear permeability coefficient, k, varies between 0.0036 and 0.0085 cm/s, and for very coarse soils it ranges from 0.0048 to 0.0093 cm/s.

Table 5 Darcy seepage equations and threshold of hydraulic gradients

Deposit	Soil type	Darcy seepage equation	J_1	J_2
1	①	$v = 0.0054J$	0.6	1.4
	②	$v = 0.0061J$	0.5	1.2
2	①	$v = 0.0036J$	0.65	1.4
	②	$v = 0.0048J$	0.6	1.3
3	①	$v = 0.0051J$	0.7	1.5
	②	$v = 0.0058J$	0.6	1.2
4	①	$v = 0.0085J$	0.6	1.3
	②	$v = 0.0093J$	0.5	1.1

Notes: J_1 - Threshold hydraulic gradient between Darcy and non-Darcy seepage; J_2 - Threshold hydraulic gradients for seepage failure; v - seepage velocity (cm/s); ① - coarse soil; ② - very coarse soil.

The test results reveal two thresholds: 1) the hydraulic gradient threshold (J_1) between linear permeability and nonlinear permeability and the seepage failure hydraulic gradient threshold (J_2). For the same deposit, J_1 *and* J_2 are generally smaller in very coarse soils than in coarse soils.

Izbash's general nonlinear permeability coefficient k_w in Equation 5 and the derived Forchheimer's k in Equation 4 are shown in Table 6. The parameter, a, for coarse soils is about 51 - 126, and about 74 - 111 for very coarse soils, respectively. The parameter b for coarse soil is about 13,550 - 70,836, and 7,980 - 39,702 for very coarse soils. The value b shows large differences between soils. The Forchheimer's k is about 0.0087 - 0.0195 cm/s for coarse soils, and 0.009 - 0.0134 cm/s for very coarse soils. The value of parameter m in Equation 5 is about 0.57 - 0.65 for coarse soils and 0.6 - 0.7 for very coarse soils. Izbash's general permeability coefficient k_w is about 0.003 - 0.0069 cm/s for coarse soils, and about 0.0039 - 0.0074 cm/s for very coarse soils.

As shown in Figures 6 and 7, permeable capacity (Part 2) at nonlinear stage appears less than that at linear stage (Part 1 in Figures 6 and 7). This is possibly due to fine particles, which are displaced by seepage flow to clog seepage channels in the sample. Another observation is that the Forchheimer's non-linear permeability coefficient, k, at the second stage (Part 2) are greater than the Darcy's permeability coefficient at the first stage (Part 1), while the Izbash's permeability coefficient, k_w is less than Darcy's one. The nonlinear seepage equation derived from Izbash's law (Table 7) is

Table 6 Equations for non-Darcy seepage

Deposit	Soil type	Forchheimer			Izbash		
		Seepage equation $J = av + bv^2$	k cm/s	R^2	Seepage equation $v = k_w J^m$	k_w cm/s	R^2
1	①	$J = 114.65v + 25834v^2$	0.0087	0.985	$v = 0.0044J^{0.6498}$	0.0044	0.991
	②	$J = 110.96v + 19983v^2$	0.009	0.988	$v = 0.0048J^{0.6667}$	0.0048	0.989
2	①	$J = 125.54v + 70836v^2$	0.008	0.991	$v = 0.003J^{0.6117}$	0.003	0.993
	②	$J = 98.286v + 39702v^2$	0.01	0.995	$v = 0.0039J^{0.6064}$	0.0039	0.993
3	①	$J = 64.236v + 37050v^2$	0.0156	0.992	$v = 0.0044J^{0.5691}$	0.0044	0.991
	②	$J = 86.866v + 27716v^2$	0.0115	0.981	$v = 0.0046J^{0.5982}$	0.0046	0.984
4	①	$J = 51.237v + 13550v^2$	0.0195	0.991	$v = 0.0069J^{0.6108}$	0.0069	0.99
	②	$J = 74.457v + 7980v^2$	0.0134	0.994	$v = 0.0074J^{0.6946}$	0.0074	0.994

Table 7 Characteristic grain sizes for permeability of the deposits

Deposit	Soil type	Permeability coefficient k (cm/s)	Viscosity coefficient υ ($\times 10^{-3}$ Pa·s)	Porosity n	Characteristic grain size d (mm)
1	①	0.0054	1.002	0.187	0.030399
	②	0.0061	1.002	0.2	0.031241
2	①	0.0036	1.002	0.194	0.024397
	②	0.0048	1.002	0.213	0.026879
3	①	0.0051	1.002	0.231	0.026593
	②	0.0058	1.002	0.2	0.030463
4	①	0.0085	1.002	0.30	0.030076
	②	0.0093	1.002	0.275	0.032875

Note: ① - coarse soil; and ② - very coarse soil therefore considered more suitable for permeability of fluvio-glacial deposits.

4.2 Correlations between permeability and sediment properties

The factors influencing permeability of coarse soils and very coarse soils are mainly particle size, shape, gradation and porosity of soils. Li (2004) suggested that there is a characteristic particle size closely relating to soil's permeability.

$$k \propto d^{m} \quad (6)$$

where k is the permeability coefficient; d characteristic particle diameter; and m is a constant.

Terzaghi (1967) proposed the following relation.

$$k = 2d_{10}^{2}e^{2} \quad (7)$$

where k is the permeability coefficient; d_{10} effective grain size; and e porosity ratio.

Yu et al. (1993), Kamann et al. (2007), and Ferreira et al. (2010) proposed the Kozeny-Carman formula.

$$k = \frac{d}{180}\frac{n^{3}}{(1-n)^{2}} \quad (8)$$

where k is the permeability coefficient; d characteristic grain size; and n porosity.

The actual seepage velocity can be obtained by the Poiseuille's seepage model:

$$v' = nv = kJ \quad (9)$$

where v' is the actual seepage velocity; k permeability coefficient; v mean seepage velocity; and n the porosity. Combining Equation 2 and Equation 9 achieves:

$$k = n\frac{d^{2}}{32}\frac{\rho g}{\upsilon} \quad (10)$$

Taking the parameter d in Equation 10 as the characteristic grain size, d may be expressed as:

$$d = \sqrt{\frac{32k\upsilon}{n\rho g}} \quad (11)$$

Equation 11 can therefore be used to determine the characteristic grain size by taking k, b, n, ρ and g as variables. The characteristic grain sizes of the studied deposits are in a narrow range between 0.024 - 0.031 mm, which is much lower than the effective grain size (d_{10}) of these deposits.

5 Conclusions

According to the investigations on the sediment properties and permeability of four Pleistocene fluvio-glacial deposits in the valley of the Dadu River, the sediments are classified into two categories, coarse soil and very coarse soil, with high density, low porosity and natural moisture content.

The permeability coefficient of the deposits obeys Darcy's law at low hydraulic gradients. However, the seepage velocity shows non-linear relation with relatively high hydraulic gradient ($J >$ 0.5 - 0.7). This nonlinear relation can be expressed as a power function as suggested by Izbash, with the constant m between 0.6 and 0.7. Seepage failure occurs after a hydraulic gradient threshold, which lies between 1.1 and 1.5 for the studied deposits.

The characteristic grain size, d, derived from this study lies between 0.024 and 0.031 mm, which matches that of silty soil or fine sands. The measured permeability coefficient falls into the range of 0.003 to 0.009 cm/s, indicating the fluvio-glacial deposits in the present study has similar permeability to silty soil or fine sands. This is possibly due to the high density and low porosity of the fluvio-glacial deposits, despite of the coarse composition.

In the present study, a special in-situ permeability test is developed, which avoids large disturbance on tested samples. However, only the shallow near surface portion (1 - 5 meters) can be sampled using the newly developed method. Despite of this, the test results together with the relations derived reveal meaningful permeability properties of the fluvio-glacial deposits. Further study in this dependency is required by sampling and testing at different depths in order to obtain an overview of the permeability characteristics of the fluvio-glacial deposits in Dadu River area.

Acknowledgements

We are very grateful to the academic and technical staff of the State Key Laboratory of Geo-hazard Prevention and Geo-environment Protection (SKLGP) of the Chengdu University of Technology, China. Thanks to Prof. Theo van Asch of Utrecht University and Dr. Huang Yanbo of The Pennsylvania State University for suggestions to improve the paper. This research is financially supported by the National Natural Fundation of China (41202212) and Independent Subject Foundation of SKLGP (SKLGP2012Z006).

References

Basak P (1976) Steady Non Darcian seepage through embankments. Journal of the Irrigation and Drainage Division 102:435-443.

Blažauskas N, Jurgaitis A, Šinkūnas P (2007) Patterns of Late Pleistocene proglacial fluvial sedimentation in the SE Lithuanian Plain. Sedimentary Geology 193:193-201.

Bordier C, Zimmer D, (2000) Drainage equations and non Darcian modeling in coarse porous media or geosynthetic macterials. Journal of Hydrology 228:174-187.

Chen X (1999) An inverse method for soil permeability estimation from gas pump tests. Computers & Geosciences 25:751-763.

Ferreira JT, Ritzi RW, Dominic DF (2010) Measuring the permeability of open-framework gravel. Ground Water 48:593-597.

Forchheimer PH (1901) Ground-water movement druch, magazine of the German Bereines ingenierre 49:1736-1749. (In German)

Hansbo S (1973). Influence of mobile particles in soft clay on permeability. Proceedings of International Symposium on Soil Structure. Goteborg: Swedish Geotechnical Institute.

Heinz J, Kleineidam S, Teutsch G, et al. (2003) Heterogeneity patterns of Quaternary glaciofluvial gravel bodies (SW-Germany): application to hydrogeology. Sedimentary Geology 158:1-23.

Hobbs WH (1931) Loess, pebble bands, and boulders from glacial outwash of the Greenland Continental glacier. The Journal of Geology 39(4):381-385.

Izbash S (1931) The filtration material in Kropnozernstom. Leningrad, USSR. (in Czechoslovakian)

Kamann PJ, Ritzi RW, Dominic DF, et al. (2007) Porosity and permeability in sediment mixtures. Ground Water 45:429-438.

Kjaer KH, Sultana L, Krüger J, et al. (2004) Architecture and sedimentation of outwash fans in front of the Mýrdalsjökull ice cap, Iceland. Sedimentary Geology 172:139-163.

Kneller B, Milana JP, Buckee C, et al. (2004) A depositional record of deglaciation in a paleofjord (Late Carboniferous [Pennsylvanian] of San Juan Province, Argentina): The role of catastrophic sedimentation. Geological Society of America Bulletin 116:348-367.

Knight J (1999) Morphology and palaeoenvironmental interpretation of deformed soft-sediment clasts: examples from within Late Pleistocene glacial outwash, Tempo Valley, Northern Ireland. Sedimentary Geology 128:293-306.

Knight J (2009) Significance of soft-sediment clasts in glacial outwash, Puget Sound, USA. Sedimentary Geology 220:126-133.

Lesaffre B (1988) Hydrologic and hydraulic operation of underground drainage temporarily congested: peak flows and SIDRA model. PhD Thesis Université Paris V1, 334p. (In French)

Li G (2004) Advanced Soil Mechanics. Tsinghua University Press, Beijing. (in Chinese)

Liu S, Cai Z, Chen J (1986) Quaternary glaciations in hte northern Hengduan Mountains. Journal of Glaciology and Geocryology 8:59-67.

Liu Y, HE Z, Wu D, et al. (2007) Geomorphic Features of the Jinchuan - Badi Sector of the Dadu River Valley. Acta Geologica Sichuan 27(3):162-165. (In Chinese)

Luo L, Yang Y (1963) Landform evolution in western Sichuan Province. Journal of Geographical Research 5:51-57.

Ministry of Transport of the People's Republic of China (2007) Test Methods of Soils for Highway Engineering. China Communication Press, Beijing. (In Chinese)

Rangeard D, Hicher PY, Zentar R (2003) Determining soil permeability from pressuremeter tests. International Journal for Numerical and Analytical Methods in Geomechanics 27:1-24.

Salem HS (2001) Application of the Kozeny-Carman equation to permeability determination for a glacial outwash aquifer, using grain-size analysis. Energy Sources 23:461-473.

Shi Y (2002) A suggestion to improve the chronology of quaternary glaciations in China. Journal of Glaciology and Geocryology 24(6): 687-692. (In Chinese)

Smerdona BD, Devitob KJ, Mendoza CA (2005) Interaction of groundwater and shallow lakes on outwash sediments in the sub-humid Boreal Plains of Canada. Journal of Hydrology 314:246-262.

Smith LN (2004) Late Pleistocene stratigraphy and implications for deglaciation and subglacial processes of the Flathead Lobe of the Cordilleran Ice Sheet, Flathead Valley, Montana, USA. Sedimentary Geology 165:295-332.

Terzaghi K, Peck RB (1967) Soil Mechanics in Engineering Practice. John Wiley and Sons Inc. New York.

Tu G (2010) Study on the engineering properties and stability of typical ancient outwash congeries in Southwestern Valley, China. PhD Dissertation, Chengdu University of Technology, China. (In Chinese)

Tu G, Deng H, Cai G (2010) Test study on the seepage properties for the transition state from laminar flow to turbulent flow in an outwash deposit. Journal of Chengdu University of Technology (Science & Technology Edition) 37(1):82-90. (In Chinese)

Tu G, Huang R, Deng H (2012) Sedimentary characteristics of the Pleistocene outwash accumulation and their implications for paleoclimate change in the midstream of Dadu River, Southwestern China. Acta Geologica Sinica(English Edition), 86(4): 924-931.

Venkataraman P, Rao PRM (2000) Validation of Forchheimer's law for flow through porous media with converging boundaries. Journal of Hydraulic Engineering 126:63-71.

Wang F, Yue X, Xu S, et al. (2009) Influence of wettability on flow characteristics of water through microtubes and cores. Chinese Science Bulletin 54:2256-2262.

Wang Y, Huang R, Duan H (2006) An intensive erosion event in the last glaciation in the west of China. Journal of Chengdu University of Technology (Science & Technology Edition) 33(1):73-76. (In Chinese)

Xiong F, Xiao Y, Zhang L (2009) An approach to developmental history of the Luding—Shimian sector of the Dadu River Valley. Acta Geologica Sichuan 29(4):379-383. (In Chinese)

Xu L, Zhou S (2009) Quaternary glaciations recorded by glacial and fluvial landforms in the Shaluli Mountains, Southeastern Tibetan Plateau. Geomorphology 103: 268-275.

Xu Q, Chen W, Jin H (2010) Characteristics and distribution of thick overburdens along the Dadu River valley. Quaternary Science 30(1):30-36. (In Chinese)

Yi C, Cui Z, Xiong H (2005) Numerical Periods of Quaternary Glaciations in China. Quaternary Sciences 25(5): 609-619. (In Chinese)

Yu A, Standish N, McLean A (1993) Porosity calculation of binary mixtures of nonspherical particles. Journal of American Ceramic Society 76(11): 2813-2816.

Zheng B (2001) Study on the Quaternary glaciation and the formation of the Moxi Platform in the east slopes of the Mount Gongga. Journal of Glaciology and Geocryology 23(3): 283-291. (In Chinese)